IRAQI JOURNAL OF APPLIED PHYSICS
Vol. 22, No. 1, January-March 2026, pp. 24-30

Effect of Annealing on Optical and Electrical Properties of ZnO Film Deposited by Thermal Spraying Technique

Rusl F. Abdalkareem [1]
Ghufran J. Matrood [2*]
Niveen J. Abdulkader [3]

[1] Al-Khadhra Secondary School for Distinguished, Ministry of Education, Baghdad, IRAQ
[2] Technical Engineering College, Middle Technical University, P.O. Box 10001, Baghdad, IRAQ
[3] College of Materials Engineering, University of Technology-Iraq, Alsina'a Street 10066, Baghdad, IRAQ
* Corresponding author: ghufranjasim@mtu.edu.iq

Zinc oxide (ZnO) thin films were effectively grown onto glass substrates via the flame spray method. The ZnO films were subsequently annealed at various temperatures (350°C, 400°C, 450°C, and 500°C). The structure and optical characteristics of the prepared films were studied by scanning electron microscope (SEM) and X-ray diffraction (XRD) techniques. The optical properties of the films were characterized by UV-visible and photoluminescence (PL) spectroscopy. Optical conductivity and optical transmittance increase with increasing annealing temperature. The photoluminescence (PL) analysis exhibited a significant enhancement in UV emission and a reduction in visible defect-related emissions at higher annealing temperatures, particularly at 500°C. Electrical resistivity decreases with an increase in annealing temperature. The annealing temperature is crucial in tuning the optoelectronic properties of ZnO films, with 500°C identified as the optimal temperature for achieving high optical conductivity, making these films well-suited for optoelectronic and sensing applications.

Keywords: Zinc oxide; Thermal Spraying; Coatings; Optical properties
Received: 4 May 2025; Revised: 9 July; Accepted: 16 July 2025; Published: 1 January 2026

1. Introduction

Zinc oxide (ZnO) nanomaterials have gained significant attention in recent years due to their promising applications in various technological fields, including electronics, photonics, catalysis, lighting, and chemical sensing. These applications of ZnO stem from its chemical stability, direct bandgap of 3.37 eV, non-toxic nature, and availability, and most importantly, the considerably strong exciton binding energy of 60 meV that ZnO possesses [1,2].

A wide array of physical and chemical ZnO synthesis methods exist to obtain thin films, including physical vapor deposition which includes sputtering [3], molecular beam epitaxy [4] and ablation with a laser [5]. There are also numerous chemical methods such as: spray pyrolysis [6], deposition from vapor phase (CVD) [7], sol gel method [8], spin coating [9], dip coating [10], and electrodeposition [11]. Of these methods, spray pyrolysis proved to be very useful in manufacturing films in favorable sizes. Its merits include ease of use, low cost, minimal processing temperatures, and great adhesion of the film to the substrate [12].

The properties of ZnO thin films prepared by spray pyrolysis are influenced by several key parameters, such as the chemical composition and concentration of the precursor solution, nozzle-to-substrate distance, spray temperature, substrate uniformity, deposition rate, and post-deposition annealing conditions [13]. This technique has been successfully employed to deposit various metal oxide films including ZnO [14], CdO [15], TiO_2 [16], SnO_2 [17], NiO [18], and Bi_2O_3 [19] on inexpensive substrates.

Spray pyrolysis involves spraying a solution of metal salts (usually in water or alcohol) onto a heated substrate, where thermal decomposition results in the formation of a metal oxide film. Substrate temperature significantly affects film morphology, potentially transforming the film structure from cracked to porous as the temperature increases [20]. Additionally, precursor type and dopant concentration are crucial in tailoring the structural and optical characteristics of the resulting film [21].

As-deposited ZnO films often exhibit high electrical resistivity, low surface roughness, and limited transparency due to poor crystallinity and residual organic materials [22–25]. These limitations can be mitigated through post-deposition treatments such as plasma treatment, laser annealing, or thermal annealing, the latter being the most widely used and effective technique [26,27]. Thermal annealing alters the film's stoichiometry and crystal structure by reducing defect states such as dislocations, oxygen and zinc vacancies, and interstitials [28–30].

Previous studies have explored the structural, optical, and electrical characteristics of ZnO thin films

prepared using different precursors and annealing conditions [31–36]. However, a comprehensive investigation into how thermal annealing temperatures affect ZnO films deposited via spray pyrolysis remains limited. Therefore, this study focuses on examining the influence of various annealing temperatures on the structural, morphological, optical, and PL properties of ZnO thin films deposited using flame thermal spraying.

2. Experimental Procedure

ZnO thin films were deposited on glass substrates using a flame thermal spray technique. First fully cleansed for deposition, the substrates underwent a 20-minute ultrasonic treatment. To eliminate any remaining metal ions or surface impurities, the substrate is immersed for 12 hours in a 0.1 M hydrochloric acid solution. After that, ZnO particles are fed into the flame to semi-melt, and then compressed air atomizes the ZnO semi-molten particles, which are then deposited on the glass substrate to form a layer of ZnO by two torch flame spray. Cold air was used on the substrate to keep the substrate from being superheated. The thermal spray setup included an oxy-acetylene flame system mounted on a motorized two-dimensional platform. This setup allowed controlled linear and vertical movement of the spray nozzle through stepper motors and screw-driven mechanisms. During deposition, the sample was fixed on a stationary platform located 100 mm away from the nozzle. The operating gas pressures were maintained at 0.5 bar for oxygen and 1 bar for acetylene, and each spray cycle lasted approximately 30 seconds. After deposition, the films were subjected to thermal annealing in ambient air at temperatures of 350, 400, 450, and 500°C for 2 hours to study the effect of post-deposition heat treatment.

Scanning electron microscopy (SEM) was used to investigate the morphologies and grain sizes of the films. Bruker X-ray diffraction (XRD) using CuKα radiation was used to analyze the crystallinity of the films. An HMS3000 manual Hall effect measurement system was used to measure the electrical resistivity of the films. Light absorption or transmission by a substance in the ultraviolet and visible spectral regions is determined using UV-visible spectroscopy. Photoluminescence spectroscopy refers to measuring the light emitted from a substance after it has absorbed photons or electromagnetic radiation.

3. Results and Discussion

Figure (2) illustrates the surface morphologies of the ZnO film deposited by flame thermal spray. The SEM micrograph of the 500°C annealed ZnO film, nearly spherical with average diameters in the range 45–62 nm. The grain boundaries are clear, and the surface overall displays a significant level of cohesion, suggesting an improved grain growth process. The overall particle assembly is interconnected, indicating improved crystallinity and decreased porosity. Surface defects and microcracks are absent, pointing to the effective healing of lattice irregularities during the annealing treatment. Such morphological characteristics, homogeneous grain sizes, good intergranular bonding, and a smooth defect-free surface are consistent with improved optical and electrical performance in ZnO thin films after annealing.

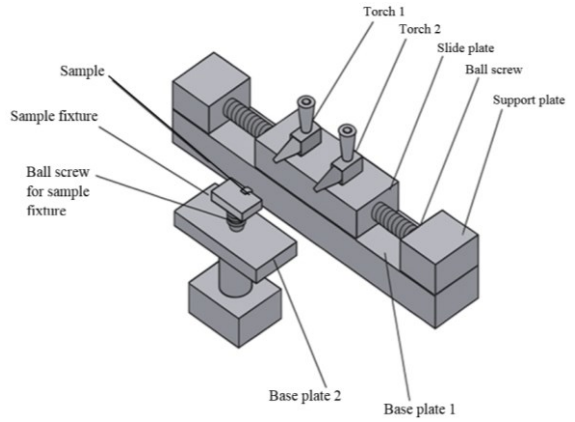

(a)

(b)

Fig. (1) Thermal spraying device, (a) schematic diagram of flame spray device, and (b) two-torch flame spray device

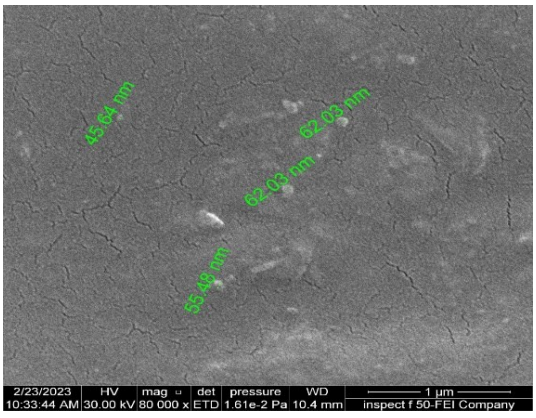

Fig. (2) Surface morphology of ZnO thin film annealed at 500°C

Figure (3) illustrates the XRD pattern for the sample. The data reveal a sequence of peaks. The planes (111), (102), (220), and (104) match 39°, 45.4°, 65°, and 78.8°. The crystalline hexagonal Wurtzite with plan orientation (102). These peaks correspond with the

conventional values of JCPDS card no. 36–1451 of ZnO. The peak intensity indicates the high crystalline quality of the produced ZnO. The crystallite size (D) can be computed using the following Scherrer's formula [37]:

$$D = \frac{0.94\lambda}{\beta cos\theta} \quad (1)$$

where β is the full-width at half maximum (FWHM), λ is the wavelength of the X-ray, and θ is Bragg's diffraction angle

The average crystallite size of ZnO film was calculated to be 36.71 nm according to the half-width of the (111) diffraction peak using the Debye-Scherrer formula.

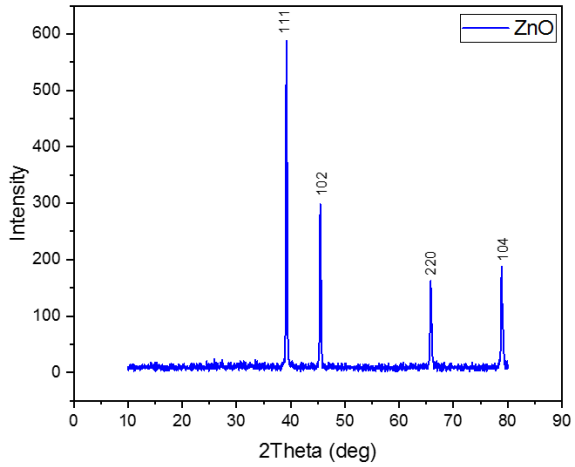

Fig. (3) XRD pattern of ZnO thin film annealed at 500°C

The UV-visible absorption spectra of ZnO thin films annealed at various temperatures are illustrated in Fig. (4). All samples exhibit a prominent absorption edge in the ultraviolet region (below 400 nm), which is characteristic of the wide bandgap of ZnO. Upon annealing, especially at 500°C (sample E), a significant increase in UV absorbance is observed, indicating improved film quality and a higher density of optically active centers. These trends are consistent with the photoluminescence results, where sample E demonstrated the strongest emission, likely due to its enhanced ability to absorb UV photons and remit them radiatively.

Figures (5) and (6) display the UV-visible optical conductivity and transmission, respectively, of ZnO films. The optical behavior of ZnO thin films was investigated under different annealing conditions (non-annealed, 350°C, 400°C, 450°C, and 500°C). Two key optical properties were analyzed: optical conductivity and transmittance (%), both as functions of wavelength. The optical conductivity increased with annealing temperature, reaching its peak at 500°C, indicating enhanced crystallinity, grain growth, and carrier mobility. This improvement is beneficial for applications requiring high electrical performance. Conversely, optical transmission decreased as the annealing temperature increased. The non-annealed film exhibited the highest transparency (~90%), while the film annealed at 500°C showed the lowest transmission (~50%), due to increased light absorption and film density. This inverse relationship between conductivity and transparency is typical for transparent conducting oxides (TCOs). Thus, the annealing temperature must be selected based on the desired application: For optoelectronic applications where conductivity is critical (e.g., UV detectors, sensors), 500°C annealing offers the best performance, and for transparent electrodes or display technologies, a compromise around 350–400°C may offer better balance between transparency and conductivity.

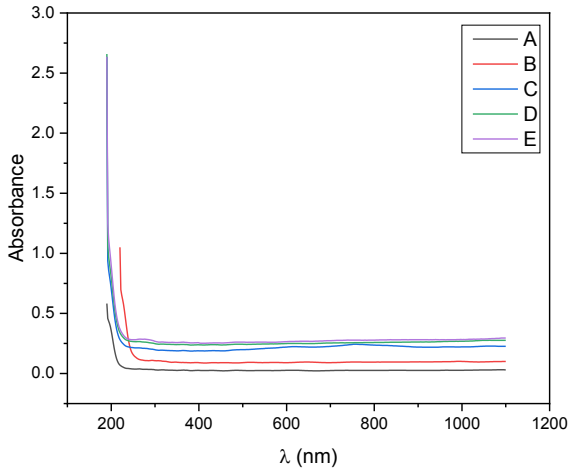

Fig (4) Absorption spectra of ZnO thin films (a) as-deposited, (b) annealed at 350°C, (c) 400°C, (d) 450°C, and (e) 500°C

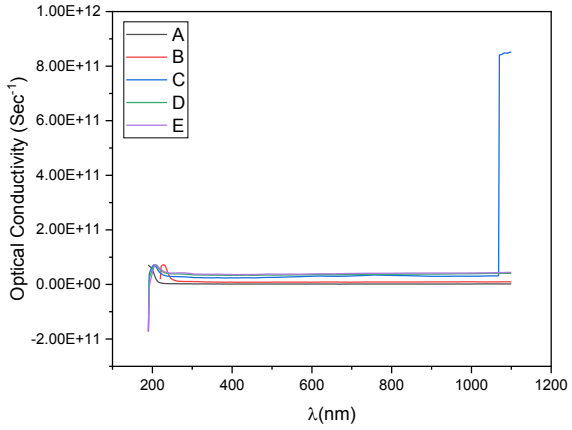

Fig. (5) Optical conductivity of ZnO thin films (a) as-deposited, (b) annealed at 350°C, (c) 400°C, (d) 450°C, and (e) 500°C

Figure (7) displays the UV-visible refractive index of ZnO thin films. The 500°C annealed ZnO film possesses the highest refractive index and thus the highest optical density because thermal energy at this temperature causes maximum grain coalescence and vacancy elimination. Physically, the bigger, well–oriented crystallites reduce void fraction and intergranular scattering, whereas oxygen vacancy and zinc interstitial elimination increase the polarizability

of bound electrons. Together, these effects increase the real part of the dielectric function ε_1, making $n=\sqrt{\varepsilon_1}$ larger. The monotonic increase in n from ~1.88 (unannealed) to ~2.04 (500°C) over 400–800 nm indicates that 500°C best balances grain-boundary removal and defect healing, with films having enhanced optical confinement and reduced sub-band-gap absorption, essential for high-performance optoelectronic devices.

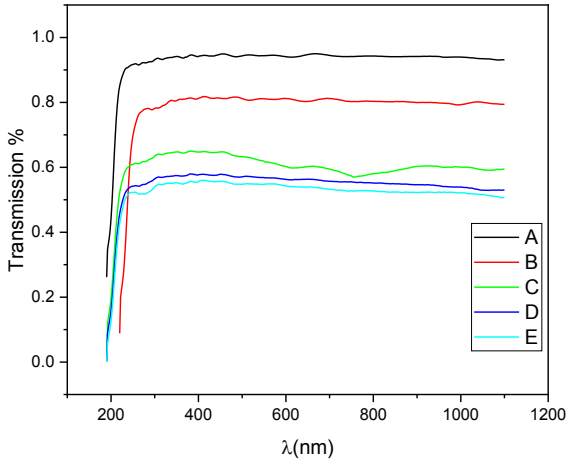

Fig. (6) Transmission spectra of ZnO thin films (a) as-deposited, (b) annealed at 350°C, (c) 400°C, (d) 450°C, and (e) 500°C

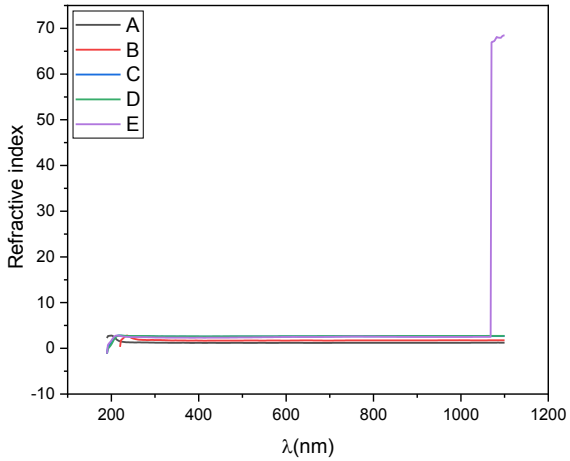

Fig. (7) Refractive index as a function of wavelength for ZnO thin films (a) as-deposited, (b) annealed at 350°C, (c) 400°C, (d) 450°C, and (e) 500°C

Figures (8) and (9) display the UV-visible real and (ε_1) imaginary (ε_2) parts of dielectric constant of ZnO thin films. Annealing ZnO films changes their dielectric behavior through the adjustment of bound-electron polarization and defect-mediated loss: real permittivity ε_1 increases with temperature from ~3.5 in films deposited as-received to ~4.2 at 500°C due to the fact that elevated thermal energy enhances grain growth, reduces porosity, and activates ions to lattice sites, all of which enhance the material's polarizability per volume. At the same time, the imaginary permittivity ε_2, which tracks sub-band-gap absorption by deep-level traps, drops as annealing recovers oxygen vacancies and zinc interstitials, reaching a minimum at 450°C; at temperatures above this, minimal stress-induced defect creation makes ε_2 rise incrementally. Physically, the 450°C treatment thus optimally balances defect elimination (optical loss reduction) and sufficient densification (ε_1 maximization), leading to films with maximum dielectric confinement and minimum parasitic absorption for high-performance optoelectronic applications.

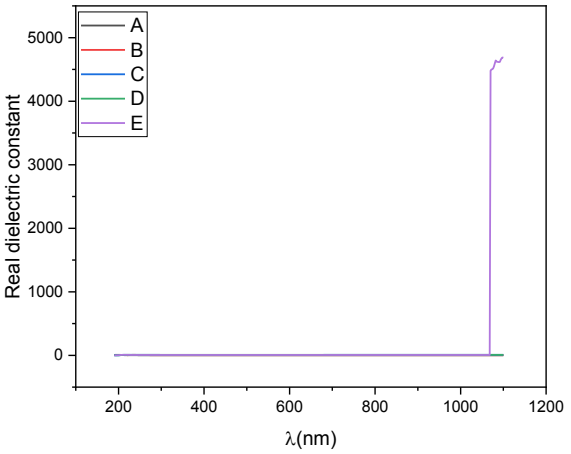

Fig. (8) Real dielectric constsnt as a function of wavelength for ZnO thin films (a) as-deposited, (b) annealed at 350°C, (c) 400°C, (d) 450°C, and (e) 500°C

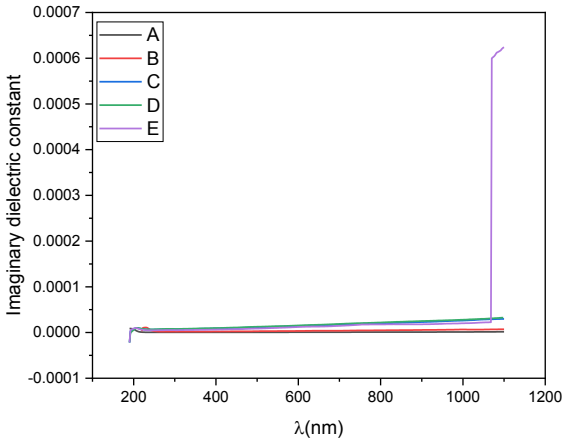

Fig. (9) Imaginary dielectric constsnt as a function of wavelength for ZnO thin films (a) as-deposited, (b) annealed at 350°C, (c) 400°C, (d) 450°C, and (e) 500°C

Figure (10) displays the UV-visible PL spectra of ZnO thin films. Analysis of Sample A reveals a very weak, broad emission at 450-500 nm, suggesting a lack of crystallinity and a high density of defect states. Following annealing at 350°C (B), there is a strong ultraviolet peak at the band edge (NBE) near 340 nm with a very much weaker defect-related band near 500 nm, indicating the onset of crystallite formation. Increased up to 400°C (C) elevates the NBE intensity (~50 mA) and shifts its peak to ~345 nm, while secondary emissions at ~450 nm and ~550 nm are

observed due to deep-level oxygen and zinc vacancies. At 450°C (D), the UV peak red-shifts to ~385 nm with strong intensity, and the green defect band (520–580 nm) becomes prominent, suggesting both effective strain relaxation and residual oxygen-vacancy centers. Finally, the 500°C anneal (E) produces the strongest NBE emission (~60 mA) at ~388 nm and strongly suppresses the mid-visible defect bands in accordance with large-scale grain growth and defect annihilation. Red-shift of the NBE peak in a systematic manner ($\lambda \approx$ 48 nm from 350 to 500°C) and corresponding increases in intensity guarantee that annealing at high temperature is mainly recovering lattice strain and promoting crystallite coarsening, hence reducing defect density and slightly narrowing the optical bandgap. Among all samples, the film annealed at 500°C shows the highest UV emission and the lowest defect luminescence and thus is the optimum condition to achieve high-quality ZnO nano-films.

Figure (11) illustrates the electrical resistivity of ZnO thin films as a function of various annealing temperatures. The electrical resistivity is significantly affected by such annealing temperatures. The resistivity of the films increases with an increase in the annealing temperature. This may be either because of the decrease in the carrier mobility or the increase in the number of the charge carriers. The rise of the annealing temperature is associated with the development of grain sizes, hence resulting in the rise of mobility variation as noted in existing literature [38,39]. The ZnO charge carriers are few at room temperature. However, upon rising temperature, there is a rise in electronically active carriers, thereby resulting in the excess of the carriers in the conduction band. The improvement observed in the carriers is because of thermal excitation, which raises the conductivity of the films. The same has been observed in the literature [40-42].

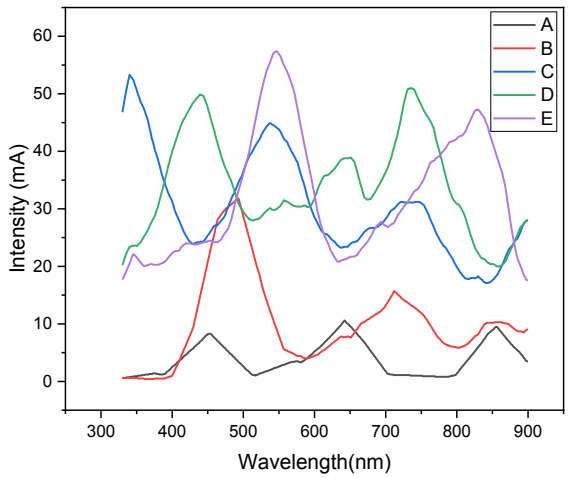

Fig. (10) PL spectra of ZnO thin films (a) as-deposited, (b) annealed at 350°C, (c) 400°C, (d) 450°C, and (e) 500°C

4. Conclusion

Thin films of ZnO were deposited onto glass substrates using the flame thermal spray technique and thermally annealed at different temperatures. The XRD showed the film was growth in the (102) direction with crystalline hexagonal wurtzite structure. The electrical resistivity of films reduces with increasing the annealing temperature. This can be attributed to either a rise in mobility or a rise in the number of carriers. Thermal annealing systematically enhances ZnO film performance by promoting grain coalescence and defect healing, which sharpens the UV–visible absorption edge, raises optical conductivity, increases refractive index and real dielectric constant, and narrows the Urbach tail to minimize imaginary dielectric constant. While 450°C yields the lowest dielectric losses for ultra-low-loss optoelectronics, 500°C delivers the highest optical density and refractive index for maximum light–matter interaction.

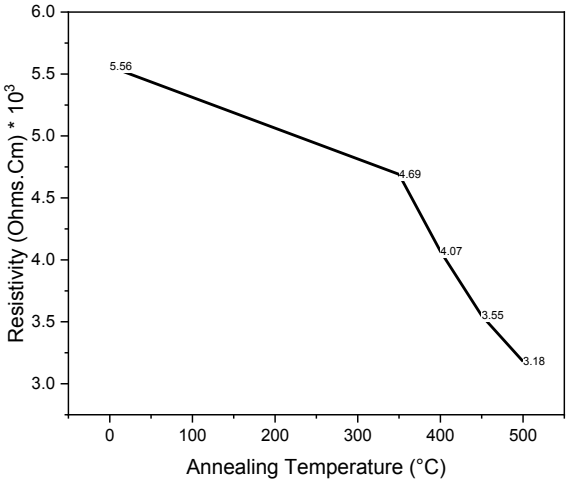

Fig. (11) Electrical resistivity variation of ZnO thin film on glass substrate as a function of annealing temperatures

References

[1] L.C. Nehru, M. Umadevi and C. Sanjeeviraja, "Studies on Structural, Optical and Electrical Properties of ZnO Thin Films Prepared by the Spray Pyrolysis Method", *Int. J. Mater. Eng.*, 2(1) (2012) 12–17.

[2] Z. Ye et al., "Structural and photoluminescent properties of ternary $Zn_{1-x}Cd_xO$ crystal films grown on Si (111) substrates", *J. Cryst. Growth*, 256(1–2) (2003) 78–82.

[3] S. Eisermann et al., "Sputter deposition of ZnO thin films at high substrate temperatures", *Thin Solid Films*, 517(20) (2009) 5805–5807.

[4] D.C. Look et al., "Characterization of homoepitaxial p-type ZnO grown by molecular beam epitaxy", *Appl. Phys. Lett.*, 81(10) (2002) 1830-1832.

[5] M. Hiramatsu et al., "Transparent conducting ZnO thin films prepared by XeCl excimer laser

ablation", *J. Vac. Sci. Technol. A: Vac. Surf. Films*, 16(2) (1998) 669–673.
[6] R. Ayouchi et al., "Preparation and characterization of transparent ZnO thin films obtained by spray pyrolysis", *Thin Solid Films*, 426(1–2) (2003) 68–77.
[7] S. Fay et al., "Low pressure chemical vapour deposition of ZnO layers for thin-film solar cells: temperature-induced morphological changes", *Sol. Ener. Mater. Sol. Cells*, 86(3) (2005) 385–397.
[8] D. Bao, H. Gu and A. Kuang, "Sol-gel-derived c-axis oriented ZnO thin films", *Thin Solid Films*, 312(1–2) (1998) 37–39.
[9] G. Srinivasan et al., "Influence of post-deposition annealing on the structural and optical properties of ZnO thin films prepared by sol–gel and spin-coating method", *Superlat. Microstruct.*, 43(2) (2008) 112–119.
[10] C.J. Brinker and A.J. Hurd, "Fundamentals of sol-gel dip-coating", *J. Physique III*, 4(7) (1994) 1231–1242.
[11] E.A. Dalchiele et al., "Electrodeposition of ZnO thin films on n-Si (100)", *Sol. Ener. Mater. Sol. Cells*, 70(3) (2001) 245–254.
[12] D. Perednis and L.J. Gauckler, "Thin film deposition using spray pyrolysis", *J. Electroceram.*, 14 (2005) 103–111.
[13] G. Korotcenkov et al., "Possibilities of aerosol technology for deposition of SnO_2-based films with improved gas sensing characteristics", *Mater. Sci. Eng. C*, 19(1–2) (2002) 73–77.
[14] M. Krunks and E. Mellikov, "Zinc oxide thin films by the spray pyrolysis method", *Thin Solid Films*, 270(1–2) (1995) 33–36.
[15] O. Vigil et al., "Structural and optical properties of annealed CdO thin films prepared by spray pyrolysis", *Mater. Chem. Phys.*, 68(1–3) (2001) 249–252.
[16] C. Natarajan, N. Fukunaga, and G. Nogami, "Titanium dioxide thin film deposited by spray pyrolysis of aqueous solution", *Thin Solid Films*, 322(1–2) (1998) 6–8.
[17] V. Brinzari, G. Korotcenkov, and V. Golovanov, "Factors influencing the gas sensing characteristics of tin dioxide films deposited by spray pyrolysis: understanding and possibilities of control", *Thin Solid Films*, 391(2) (2001) 167–175.
[18] P.S. Patil and L.D. Kadam, "Preparation and characterization of spray pyrolyzed nickel oxide (NiO) thin films", *Appl. Surf. Sci.*, 199(1–4) (2002) 211–221.
[19] T.P. Gujar, V.R. Shinde and C.D. Lokhande, "Spray pyrolysed bismuth oxide thin films and their characterization", *Mater. Res. Bull.*, 41(8) (2006) 1558–1564.
[20] P.J.J.M. ávan der Put, "Morphology control of thin $LiCoO_2$ films fabricated using the electrostatic spray deposition (ESD) technique", *J. Mater. Chem.*, 6(5) (1996) 765–771.
[21] S. Golshahi et al., "P-type ZnO thin film deposited by spray pyrolysis technique: The effect of solution concentration", *Thin Solid Films*, 518(4) (2009) 1149–1152.
[22] S. Salam et al., "The effect of processing conditions on the structural morphology and physical properties of ZnO and CdS thin films produced via sol–gel synthesis and chemical bath deposition techniques", *Adv. Nat. Sci.: Nanosci. Nanotech.*, 2(4) (2011) 045001.
[23] X. Zhu et al., "Preferential growth and enhanced dielectric properties of $Ba_{0.7}Sr_{0.3}TiO_3$ thin films with preannealed Pt bottom electrode", *J. Phys. D. Appl. Phys.*, 46(10) (2013) 105301.
[24] A.A. Hameed and M.M. Khalaf, "Extraction of Zinc oxide Nanopowders Prepared by Physical Vapor Deposition Technique", *Iraqi J. Appl. Phys. Lett.*, 7(1) (2024) 3-6.
[25] J. Karamdel, C.F. Dee and B.Y. Majlis, "Effects of annealing conditions on the surface morphology and crystallinity of sputtered ZnO nano films", *Sains Malays.*, 40(3) (2011) 209–213.
[26] A.J. Faraj and K.O. Salman, "Low-Pressure Pulsed-Laser Deposition of ZnMgO Nanostructures from Sputtered Zn-Coated Mg Target", *Iraqi J. Mater.*, 4(3) (2025) 125-130.
[27] J. Yang, J. Bei, and S. Wang, "Enhanced cell affinity of poly (D, L-lactide) by combining plasma treatment with collagen anchorage", *Biomater.*, 23(12) (2002) 2607–2614.
[28] B. Du Ahn et al., "Influence of thermal annealing ambient on Ga-doped ZnO thin films", *J. Cryst. Growth*, 309(2) (2007) 128–133.
[29] H.S. Kang et al., "Annealing effect on the property of ultraviolet and green emissions of ZnO thin films", *J. Appl. Phys.*, 95(3) (2004) 1246–1250.
[30] P. Sagar et al., "Photoluminescence and absorption in sol–gel-derived ZnO films", *J. Lumin.*, 126(2) (2007) 800–806.
[31] P. Nunes, E. Fortunato and R. Martins, "Influence of the post-treatment on the properties of ZnO thin films", *Thin Solid Films*, 383(1–2) (2001) 277–280.
[32] P. Nunes et al., "Performances presented by zinc oxide thin films deposited by spray pyrolysis", *Thin Solid Films*, 337(1–2) (1999) 176–179.
[33] K.H. Yoon and J.Y. Cho, "Photoluminescence characteristics of zinc oxide thin films prepared by spray pyrolysis technique", *Mater. Res. Bull.*, 35(1) (2000) 39–46.
[34] R. Ayouchi et al., "Growth of pure ZnO thin films prepared by chemical spray pyrolysis on silicon", *J. Cryst. Growth*, 247(3–4) (2003) 497–504.

[35] A.R. Bagheri and S. Ibrahimi, "Enhancement of Photoluminescence Characteristics of Zinc Oxide Nanostructures Using Inclined Pulsed Laser Irradiation", *Iraqi J. Appl. Phys. Lett.*, 8(1) (2025) 17-20.

[36] A. Jehanbaksh and A.A. ferzadpoor, "Photoluminescence Characteristics of Gold-decorated Zinc Oxide Nanostructures Synthesized by Pulsed-Laser Deposition", *Iraqi J. Appl. Phys. Lett.*, 8(4) (2025) 119-122.

[37] M. Ladd and R. Palmer, "Structure Determination by X-ray Crystallography", 5th ed., Springer (NY, 2013), p. 585.

[38] G.J. Matrood, N.J. Abdulkader and N.M. Ali, "Determination of electrical conductivity of aluminum nano films prepared by flame thermal spray", *Iraqi J. Appl. Phys.*, 20(2B) (2024) 453–456.

[39] S. Chen et al., "Growth methods, enhanced photoluminescence, high hydrophobicity and light scattering of 4, 4′-bis (1, 2, 2-triphenylvinyl) biphenyl nanowires", *Org. Electron.*, 13(10) (2012) 1996–2002.

[40] Q. Humayun, M. Kashif and U. Hashim, "Area-selective ZnO thin film deposition on variable microgap electrodes and their impact on UV sensing", *J. Nanomater.*, 2013 (2013) Article 301674.

[41] M. Rusop et al., "Post-growth annealing of zinc oxide thin films pulsed laser deposited under enhanced oxygen pressure on quartz and silicon substrates", *Mater. Sci. Eng. B*, 127(2-3) (200) 150-153.

[42] N.H. Al-Hardan et al., "ZnO thin films for VOC sensing applications", *Vacuum*, 85(1) (2010) 101–106.

